

The Moment of Inertia and the Scissors Mode of a Bose-condensed Gas

O.M. Maragò, G. Hechenblaikner, E. Hodby, S.A. Hopkins and C.J. Foot

Clarendon Laboratory, Department of Physics, University of Oxford,
Parks Road, Oxford, OX1 3PU, United Kingdom.

Abstract. We relate the frequency of the scissors mode to the moment of inertia of a trapped Bose gas at finite temperature in a semi-classical approximation. We apply these theoretical results to the data obtained in our previous study of the properties of the scissors mode of a trapped Bose-Einstein condensate of ^{87}Rb atoms as a function of the temperature. The frequency shifts that we measured show quenching of the moment of inertia of the Bose gas at temperatures below the transition temperature - the system has a lower moment of inertia than of a rigid body with the same mass distribution, because of superfluidity.

PACS numbers: 03.75.Fi, 05.30.Jp, 32.80.Pj, 67.90.+z

1. INTRODUCTION

The onset of Bose-Einstein condensation [1] (BEC) in ultra-cold atomic gases is clearly observed through the change in the density profile of the confined system. On the contrary superfluid behavior in these systems has proved to be more difficult to observe. Four years after the first observation of BEC in atomic gases, evidence for superfluidity was ‘still quite circumstantial’ [2] but in recent years superfluid phenomena in dilute gases have been the subject of much theoretical and experimental work [3]. Superfluidity in trapped condensates was clearly demonstrated by experiments that showed evidence for a critical velocity [4], the creation of vortices [5, 6] and the observations of the scissors mode [7, 8]. Many striking features of superfluids are associated with their response to rotation. In this paper we concentrate only on one aspect, namely the quenching of the moment of inertia, so that the superfluid always has less moment of inertia than a rigid body with same density distribution. We first review our recent results on the scissors mode of excitation, which is our tool to measure the moment of inertia of the Bose gas. We then use the theory recently developed by Zambelli and Stringari [9] to deduce the moment of inertia of the gas at finite temperature.

2. THE SCISSORS MODE

The scissors mode of excitation was first studied in atomic nuclei and predicted by a geometrical model [10]. Its experimental discovery [11] has been one of the most exciting findings in nuclear physics during the last two decades [12]. According to the geometrical picture, such a mode arises from a counter-rotational oscillation of the deformed proton and neutron fluids, where the axes of the deformed clouds move like the blades of a pair of scissors. Extensive studies of this mode have investigated important features such as the dependence of its strength on the nuclear deformation and its relation with the superfluid moment of inertia of the nucleus [12].

In a theoretical paper [7] D. Guéry-Odelin and S. Stringari extended the study of the scissors mode to the case of trapped gases. They investigated the oscillatory excitation of a dilute atomic gas following a sudden rotation of the anisotropic confining potential and they showed how the scissors mode is a manifestation of the superfluidity of a trapped BEC. In this section we apply their approach to the specific geometry of our TOP trap and discuss the expected results for the scissors mode of both the BEC and the classical gas. We then show experimental results for the scissors mode oscillations and finally put the scissors mode into the context of the low-energy spectrum of BEC excitations.

A Bose condensate of density $n(\vec{r}, t)$ at $T = 0$ is well described by the hydrodynamic equations of superfluids:

$$\frac{\partial n}{\partial t} + \nabla \cdot (n\vec{v}) = 0 \quad \text{Continuity Equation} \quad (1)$$

$$m \frac{\partial \vec{v}}{\partial t} + \nabla \left(V_{ext} + gn + \frac{mv^2}{2} \right) = 0 \quad \text{Force Equation} \quad (2)$$

where V_{ext} is the external potential, g characterizes the particle interaction strength and m is the mass of the particles. The velocity flow $\vec{v}(\vec{r}, t)$ is related to the phase $S(\vec{r}, t)$ of the complex order parameter $\Phi = \sqrt{n} e^{iS}$ through:

$$\vec{v}(\vec{r}, t) = \frac{\hbar}{m} \nabla S(\vec{r}, t). \quad (3)$$

This relation immediately leads to $\nabla \times \vec{v} = 0$, i.e. the velocity flow is irrotational. Since Φ must be single-valued the phase change over a closed path must be modulo 2π . In the case of a BEC with a large number of atoms, we can use the Thomas-Fermi ground state density distribution $n = [\mu - V_{ext}(\vec{r})]/g$ as a stationary solution [13], where μ is the chemical potential.

The gas is initially in thermal equilibrium in an anisotropic harmonic potential $V_{ext}(r)$ with three frequencies $\omega_x \simeq \omega_y < \omega_z$

$$V_{ext}(r) = \frac{m}{2} (\omega_x^2 x^2 + \omega_y^2 y^2 + \omega_z^2 z^2). \quad (4)$$

It is convenient to define the two quantities $\omega_{sc} = \sqrt{\omega_x^2 + \omega_z^2}$ and $\epsilon = (\omega_z^2 - \omega_x^2)/(\omega_z^2 + \omega_x^2)$ where ϵ gives a measure of the deformation of the confining potential. For the TOP trap case we have $\omega_z = \sqrt{8}\omega_x$, so that $\omega_{sc} = 3\omega_x$ and $\epsilon = 7/9$. To start the scissors

mode at a certain time one rotates the trapping potential through a small angle θ_0 about the y axis. The condensate is no longer in equilibrium and the atomic cloud will start oscillating about the y axis. After the sudden rotation of the trapping potential the TF density can be rewritten with respect to axes of the rotated potential. Making the small angle approximations $x \rightarrow x - \theta z$ and $z \rightarrow z + \theta x$, leads to a time-dependent density:

$$n(\vec{r}, t) = \frac{\mu}{g} - \frac{m}{2g} [\omega_x^2 x^2 + \omega_y^2 y^2 + \omega_z^2 z^2 + 2\omega_{sc}^2 \epsilon \theta(t) xz] \quad (5)$$

In the subsequent motion, the cloud is not deformed provided that the change in the potential is too small to excite shape oscillations. In other words the scissors motion is completely decoupled from ‘compressional’ modes and the velocity flow satisfies the condition

$$\nabla \cdot \vec{v} = 0. \quad (6)$$

The velocity flow for a condensate is also irrotational. The constraints on the velocity flow lead to

$$\vec{v} = \beta(t) \nabla(xz). \quad (7)$$

Substituting the expressions for n and \vec{v} into Eqs. 1 and 2 we then get two equations for the angle $\theta(t)$ and the phase parameter $\beta(t)$:

$$\begin{cases} \dot{\theta}(t) &= -\beta(t)/\epsilon \\ \dot{\beta}(t) &= \omega_{sc}^2 \epsilon \theta(t) \end{cases} \quad (8)$$

Oscillations cannot occur about an axis with cylindrical symmetry i.e. $\epsilon = 0$, since in this case the angle θ loses its geometrical meaning and the phase of the condensate is constant. When $\epsilon \neq 0$, Eqs. 8 lead to harmonic angular motion of the cloud $\ddot{\theta} = -\omega_{sc}^2 \theta$. The initial conditions $\theta(0) = \theta_0$ and $\vec{v}(0) = 0$ yields the solutions:

$$\begin{cases} \theta(t) &= \theta_0 \cos(\omega_{sc} t) \\ \beta(t) &= \epsilon \theta_0 \omega_{sc} \sin(\omega_{sc} t). \end{cases} \quad (9)$$

The scissors mode is an oscillation of the condensed cloud at ω_{sc} which is undamped at $T = 0$. This result is a direct consequence of superfluidity and in particular of the relation between the velocity flow and the phase of the condensate. In this sense the constraint on the overall phase of the order parameter is transposed to the dynamical behavior of the cloud during a scissors oscillation.

The thermal gas behaves in a completely different way after a scissors excitation. In the so-called collisionless regime (when the collision time is larger than the trap oscillation period), the evolution of the cloud angle is the superposition of two undamped oscillations at frequencies given by $\omega_{\pm} = |\omega_z \pm \omega_x|$ [7]. The sudden rotation of the potential excites both low and high frequency oscillations with the same amplitude. These two modes correspond to two types of flow pattern: the high frequency one is irrotational flow whereas the low frequency oscillation is of rotational nature, related to the rigid body value for the moment of inertia of a classical gas. We can summarize these results by writing the velocity flow of the classical gas in terms of a rotational

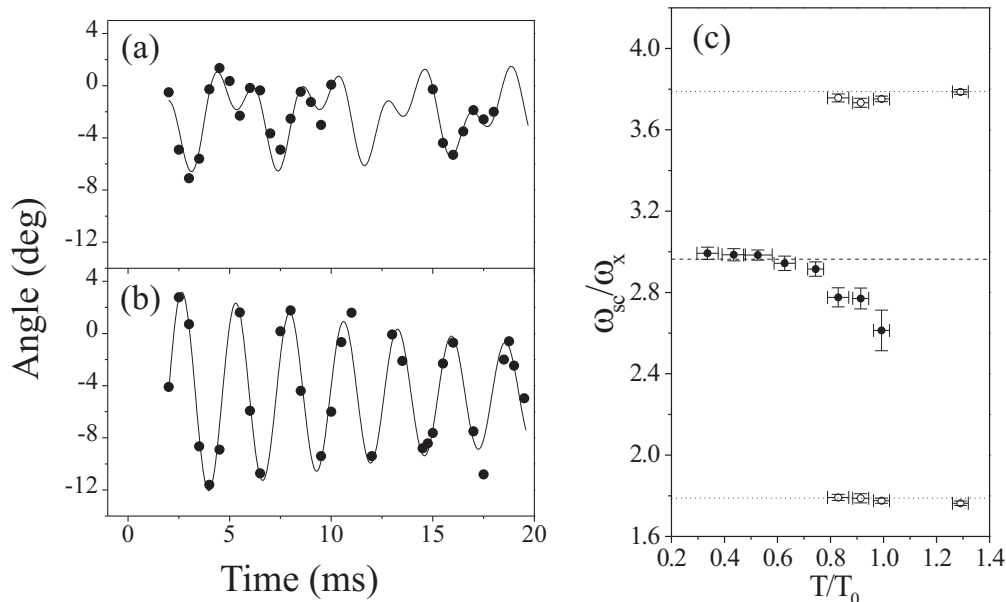


Figure 1. Scissors mode oscillations and frequency shifts (as reported in [15]). (a) Scissors oscillation of a thermal cloud at $T/T_0 = 1.29$. The scissors mode is characterized by two frequencies of oscillation with equal amplitude. (b) A condensate at $T/T_0 = 0.53$ exhibits an almost undamped oscillation at a frequency that agrees well with the hydrodynamic value. (c) Temperature dependent frequency shift of the scissors mode of the condensate (solid circles) and hydrodynamic prediction (dashed line). The low temperature frequencies are systematically higher than the hydrodynamic value by $\sim 1\%$ because of the finite number of atoms. The scissors mode frequencies of the thermal component are represented by open circles and the collisionless predictions by the dotted lines. The frequency spectrum has been normalized to ω_x .

frequency Ω_{rot} and of a scalar pseudo-potential $\chi(\vec{r})$ responsible for the irrotational flow $\vec{v} = \vec{\Omega}_{rot} \times \vec{r} + \nabla\chi(\vec{r})$ [14].

In our experiments [8, 15] we use radio-frequency induced evaporation to cool the atoms in a TOP trap to the desired temperature T (we obtain ‘pure’ condensates with 2×10^4 atoms). The frequencies of this trap are $\omega_x = \omega_y = 2\pi \times 126$ Hz, $\omega_z = \sqrt{8}\omega_x$. We then apply an oscillatory bias field along the z axis, which adiabatically tilts the confining potential by a small angle ϕ in 0.2 s. This angle was kept fixed at a value of $\phi = 3.4^\circ$ for all the measurements. This procedure also reduces ω_z by $\sim 2\%$. After the adiabatic tilting, we suddenly flip the trap angle to $-\phi$. This excites the scissors mode in the xz plane with an amplitude $\theta_0 = 2\phi$, about the new equilibrium position. To observe the scissors mode of the thermal cloud after the sudden rotation of the potential, pictures of the atom cloud in the trap were taken after a variable delay. The angle of the cloud was extracted from a 2-D Gaussian fit of the absorption profiles. To observe the scissors mode in a Bose-Einstein condensed gas we allow the BEC to evolve in the

trap for a variable time after exciting the scissors mode and then release the condensate from the trap so that it expands for 14 ms before the time-of-flight image. The repulsive mean-field interactions cause the cloud to expand rapidly when the confining potential is switched off, so that its spread is much greater than the initial size. The aspect ratio of the cloud changes during the expansion (the long axis is always at 90° to the original long axis in the trap) but this does not affect the results since we only extract the frequency at which the cloud angle oscillates.

Figure 1 shows in (a) the scissors mode oscillations for the thermal cloud ($T/T_0 = 1.29$, T_0 being the transition temperature) and in (b) for the condensate ($T/T_0 = 0.53$), in (c) we plot the scissors mode frequency shift as a function of temperature [15]. The measured frequencies of the thermal cloud do not change with temperature and agree very well with the collisionless frequencies, both above and below the critical temperature. Both frequency components have the same amplitude implying that energy is shared equally between rotational and irrotational velocity flow. The scissors mode oscillation of the BEC component occurs at a *single frequency* ω_{sc} . However, the frequency of oscillation and its damping change dramatically with temperature [15]. Figure 1 (c) shows the measured frequencies for the scissors mode of thermal cloud (open circles) and condensate (solid circles) for different temperatures. For the lower temperature BEC points we measure a frequency that is systematically $\sim 1\%$ higher than the hydrodynamic prediction. This agrees with the scissors mode frequency we calculated for a finite number condensate (2×10^4) using the method by Pires and de Passos [16]. Stimulated by our work, Jackson and Zaremba [17] have recently developed a theoretical description of the scissors mode at finite T . Their theoretical results are in good agreement with our experimental results for a wide range of temperatures. Close to the critical temperature, $T/T_0 > 0.8$, there are some discrepancies and both the frequency shift and damping rate simulations deviate from the observed behaviour.

The scissors mode is a previously unobserved collective mode of a BEC and Fig. 2 shows how it fits in with the other energy modes. The dipole modes (center of mass motion) of a BEC occur at the trap frequencies by Kohn's theorem, and we used this property to calibrate our trap frequencies. The frequencies of other collective modes do not directly correspond to harmonic oscillator states because of the atomic interactions. In an axially symmetric trap the angular momentum about the symmetry axis is conserved and we use its eigenvalue m to label the low energy modes. We have a high and low-lying $m = 0$ modes and the $m = 2$ mode [18]. Moreover there are two degenerate ($\omega_x = \omega_y$) scissors modes with frequencies $\omega_{xz} = \omega_{yz} = \omega_{sc}$.

3. MOMENT OF INERTIA

The moment of inertia is a fundamental quantity of a physical system that characterizes its rotational properties. For rotation about the z axis a classical rigid body has a moment of inertia given by $\Theta_{rig} = mN\langle x^2 + y^2 \rangle$ where N is the number of particles in the system, m their mass and $\langle \rangle$ denotes an ensemble average. In superfluids the

Spectrum of BEC in TOP

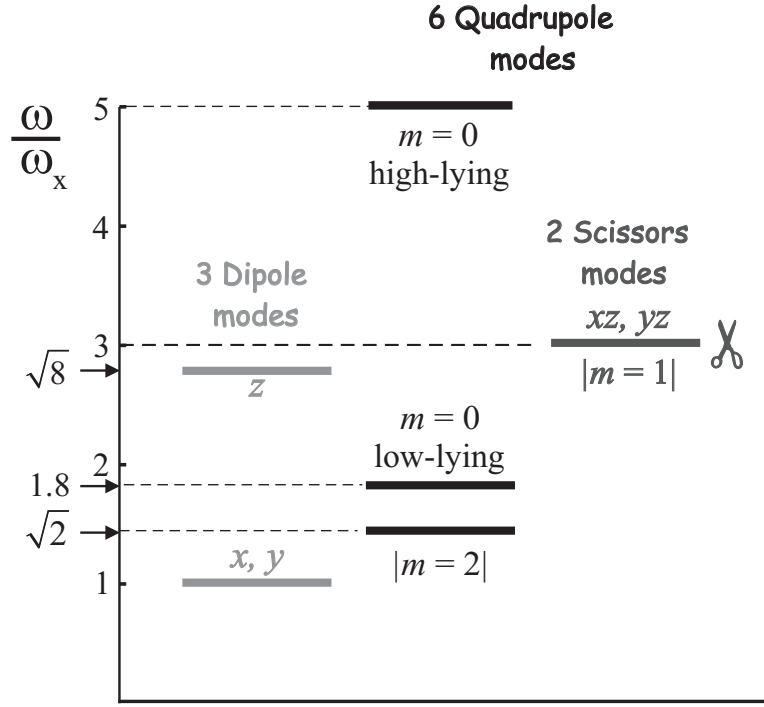


Figure 2. Low energy spectrum of a trapped BEC in a TOP trap. In a TOP trap geometry $\omega_x = \omega_y$, the z component of the angular momentum is conserved and m is a good quantum number. There are three dipole modes: one at ω_z and two degenerate modes at ω_x . The six quadrupole modes are: $m = 0$ high-lying, $m = 0$ low-lying, the doubly degenerate $|m = 2|$ and two degenerate scissors modes. In an anisotropic trap we have three dipole modes, three scissors modes (odd parity) and three compressional modes (even parity).

response to a weak rotational field is always less than that of a classical rigid body. This *quenching* of the moment of inertia have been studied in different many-body systems. In early experiments on liquid helium by Andronikashvili, measurements on the moment of inertia gave a quantitative measure of the superfluid density [19]. In nuclear physics the strong reduction of the moment of inertia with respect to the rigid body value gave indication of the superfluidity of nuclear matter soon after the discovery of nuclear rotational states [20].

In the framework of linear response theory [21] the moment of inertia of a gas Θ is a dynamical property of the system. Relative to a certain rotation axis, it is defined as the linear response to a rotational probe field $-\Omega \hat{J}_z$

$$\Theta = \lim_{\Omega \rightarrow 0} \frac{\langle \hat{J}_z \rangle}{\Omega}. \quad (10)$$

For a Bose condensed gas this definition holds for systems rotating with angular velocities less than the critical value Ω_c which gives the occurrence of quantized vortices. In our experiments we study the response to an angular impulse and the *rotational*

probe is the scissors excitation. The link between the scissors mode and the moment of inertia has been recently established by Zambelli and Stringari [9]. In their analysis they calculate explicitly the moment of inertia of the boson gas Θ using the quadrupole response function. This derivation leads to the evaluation of Θ for the condensate at $T = 0$ and the thermal cloud at $T > T_0$ directly from scissors mode frequency measurements.

Following their approach we can write the Hamiltonian of an interacting boson gas as the sum of the kinetic energy, a term that represents the two-body interaction between the particles and the confining harmonic potential $\hat{V}_{ext}(\vec{r})$ (the operator for the potential of Eq. 4). The crucial point of their analysis is the commutation relation that follows from the rotational symmetry of the internal part of the Hamiltonian (kinetic and self-interaction terms), so that:

$$[\hat{H}, \hat{J}_z] = [\hat{V}_{ext}, \hat{J}_z] = im\hbar(\omega_x^2 - \omega_y^2)\hat{Q} \quad (11)$$

where $\hat{Q} = xy$ is the quadrupole operator [22]. This equation links the dynamics of the angular momentum with the quadrupole operator that arises because of the deformation of the trap. From this important relation and from the definition of moment of inertia in the context of linear response theory it is possible to write Θ as a function of the imaginary part of the quadrupole dynamic response function [21]. Thus the occurrence of superfluidity that is responsible for the quenching of the moment of inertia is fundamentally linked to the dynamics of quadrupole excitations.

In a scissors mode experiment we have a sudden rotation of the trap through a small angle θ_0 . The resulting external time-dependent Hamiltonian comes from the angular displacement of the potential with respect to the atomic cloud and for $t > 0$ can be written as $\hat{H}_{ext}(t) = m\theta_0(\omega_x^2 - \omega_y^2)\hat{Q}$. Using linear response theory it is then possible to find the evolution of the average $Q(t) \equiv \langle \hat{Q} \rangle$ and a relation between the reduced moment of inertia and the quadrupole Fourier signal $Q(\omega)$ [9]:

$$\Theta' = (\omega_x^2 - \omega_y^2)^2 \frac{\int d\omega Q(\omega)/\omega^2}{\int d\omega Q(\omega)\omega^2}. \quad (12)$$

This important general relation allows us to extract information about the moment of inertia from the Fourier transform of the quadrupole moment. This signal in our experiment is intrinsically related to the scissors mode angle oscillation $Q(t) = N(y^2 - x^2)\theta(t)$.

The relations discussed so far are very general and do not rely on any model for the cloud density distribution. We can apply these equations in different regimes and specifically to our scissors mode data. At $T = 0$ the condensate has a single frequency scissors oscillation both for the ideal and the interacting gas. From this prediction we have that the quadrupole signal has a delta-like Fourier spectrum with amplitude $Q_{0,c} = \theta_0 N \langle y^2 - x^2 \rangle_c$ and resonant frequency $\omega_{sc}(N, T)$. Application of Eq. 12 yields:

$$\Theta'_c = \frac{(\omega_x^2 - \omega_y^2)^2}{\omega_{sc}^4(N, T)}. \quad (13)$$

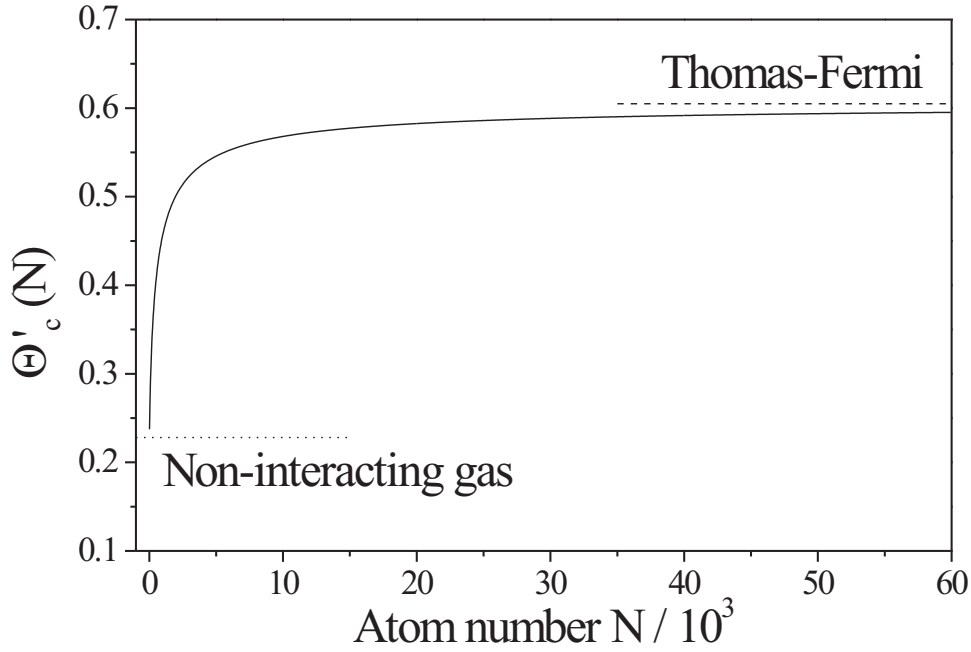


Figure 3. Moment of inertia and atom number. For very small number of atoms the moment of inertia is consistent with the $T = 0$ non-interacting gas result (dotted line) i.e. $\Theta'_{ho} = \epsilon_{ho}^2 \approx 0.23$. In the large atom number limit the moment of inertia approaches the Thomas-Fermi irrotational value (dashed line) i.e. $\Theta'_c = \epsilon^2 \approx 0.6$.

In the specific case of the TOP trap geometry we have that $\omega_x = \omega_y$ and so Θ'_c with respect to z is zero due to the rotational symmetry. The axial frequency is $\omega_z = \sqrt{8}\omega_x$ and we can consider a scissors oscillation about the y axis. In the Thomas-Fermi limit, using the expression for the scissors mode frequency defined in Sec. 2, we obtain the quenched irrotational value of the moment of inertia $\Theta'_c = \epsilon^2 \simeq 0.6$. We can also use Eq. 13 for a non-interacting condensate. In this case the scissors frequency is simply the harmonic oscillator prediction $\omega_{sc,ho} = \omega_z + \omega_x$ and we eventually obtain the ideal gas value of the moment of inertia [23] $\Theta'_{ho} = \epsilon_{ho}^2 \simeq 0.23$, where $\epsilon_{ho} = (\omega_x - \omega_y)/(\omega_x + \omega_y)$ is the deformation of the harmonic oscillator ground state. Indeed the interaction among the particles changes dramatically the rotational properties of the BEC embodied in the dynamics of the scissors mode. Therefore to evaluate this effect we can investigate the frequency change of the scissors mode with atom number [16] and make use of Eq. 13. The result of this procedure is shown in fig. 3. These calculations were made for a TOP trap with radial frequency $\omega_x/2\pi = 126$ Hz. For very low atom number, i.e. low interactions strength, we recover the ideal gas result $\Theta'_{ho} \simeq 0.23$. While in the limit of large N the moment of inertia approach the Thomas-Fermi result $\Theta'_c \simeq 0.6$.

For a collisionless thermal cloud the response to a scissors excitation exhibits two

frequencies at ω_+ and ω_- with the same amplitude $\theta_0/2$. The quadrupole signal amplitudes are related to the angle amplitude through $Q_{0,th} = N\langle y^2 - x^2 \rangle_{th}\theta_0/2$. Application of Eq. 12 yields the moment of inertia for the gas above T_0 :

$$\Theta'_{th} = \frac{(\omega_x^2 - \omega_y^2)^2}{\omega_+^2 \omega_-^2}. \quad (14)$$

Using the scissors mode collisionless frequencies we obtain the rigid body value for the moment of inertia $\Theta' = 1$ as expected for a classical gas. For the thermal cloud the occurrence of the low frequency mode at ω_- is the key feature that yields the rigid body response of the gas to the scissors excitation. For both $T = 0$ and $T > T_0$ the reduced moment of inertia only depends on the scissors mode frequencies and the geometry of the trap - it is independent of the amplitude of the oscillations. This is not the case in the intermediate regime i.e. for condensed clouds at finite temperature.

In the general case when the Bose condensed cloud exhibits a scissors motion at finite temperature the analysis of the *total* moment of inertia through the scissors oscillation becomes more complicated. Indeed the normal and superfluid component respond in a different way to the sudden rotation of the trap. However we can extend the formalism developed in [9, 23] to extract important information on the total moment of inertia in a semi-classical approximation. This approximation holds when the temperature T of the system is much larger than the harmonic oscillator energy $\hbar\omega_{ho}$. This is the case for current experiments on dilute gases and in particular for our experiment.

First of all for partially condensed clouds we need to introduce two distinct angles for the condensate $\theta_c(t)$ and the thermal cloud $\theta_{th}(t)$. Thus after the sudden rotation of the trap the time dependent density of the gas will have a time dependent contribution from both the condensed and the thermal components. We can use the semi-classical approach to evaluate the total quadrupole moment of the gas. In fact, in the linear regime $Q(t)$ is the sum of two terms, one related to the BEC and one related to the thermal cloud oscillation $Q(t) = Q_c(t) + Q_{th}(t)$ with

$$Q_c(t) = N_0(T)\langle y^2 - x^2 \rangle_c \theta_c(t) \quad (15)$$

$$Q_{th}(t) = [N - N_0(T)] \langle y^2 - x^2 \rangle_{th} \theta_{th}(t). \quad (16)$$

Where N is the total number of atoms, $N_0(T)$ is the temperature dependent number of condensed atoms, and the average $\langle \rangle_c$ and $\langle \rangle_{th}$ are evaluated over the condensate and thermal distributions respectively. The total Fourier signal will be the sum of two distinct terms as well. In particular the condensate responds at one frequency for all temperatures. Instead the thermal cloud signal is a two frequency oscillation at all temperatures (see fig. 1). Neglecting the damping we can write the Fourier quadrupole signal as a superposition of δ -like functions with temperature dependent amplitudes:

$$Q_{0,th}(T) = \frac{\theta_0 k_B T}{2m} \frac{G(3)}{3G(2)} [N - N_0(T)] \frac{\omega_x^2 - \omega_y^2}{\omega_x^2 \omega_y^2} \quad (17)$$

$$Q_{0,c}(T) = \frac{2\theta_0\mu(T)N_0(T)}{7m} \frac{\omega_x^2 - \omega_y^2}{\omega_x^2\omega_y^2}. \quad (18)$$

where $G(3) \approx 6.5$, $G(2) \approx 2.4$ are numerical coefficients [23]. Substituting the total Fourier signal $Q(\omega)$ in Eq. 12 under the conditions outlined above, we get:

$$\Theta'(T) = \frac{\Theta'_c(T) + \Theta'_{th}\mathcal{F}(N, T)}{1 + \mathcal{F}(N, T)}. \quad (19)$$

Here $\Theta'_c(T)$ and Θ'_{th} are the same as Eqs. 13 and 14 respectively but with the temperature dependent frequencies of the scissors mode. Instead the temperature dependent function $\mathcal{F}(N, T)$ is related to the signal amplitudes and takes the expression:

$$\mathcal{F}(N, T) = \frac{Q_{0,th}}{Q_{0,c}} \frac{\omega_+^2 + \omega_-^2}{\omega_{sc}^2}. \quad (20)$$

In the Thomas-Fermi limit we eventually obtain:

$$\mathcal{F}(N, T) = \frac{7k_B T}{4\mu(T)} \frac{G(3)}{3G(2)} \frac{N - N_0(T)}{N_0(T)} \frac{\omega_+^2 + \omega_-^2}{\omega_{sc}^2(T)}. \quad (21)$$

It is interesting to consider the two limiting cases for $T \rightarrow 0$ and $T \rightarrow T_0$. In the first situation we have that $\lim_{T \rightarrow 0} \mathcal{F}(N, T) = 0$ and $\Theta'(0) = \Theta'_c(0) = \epsilon^2$. While in the limit $T \rightarrow T_0$ the function $\mathcal{F}(N, T)$ diverges and we recover the rigid body value of the moment of inertia $\Theta'(T_0) = \Theta'_{th} = 1$. This result can be compared with the one obtained from the densities without considering any dynamics of the clouds [23]:

$$\Theta'(T) = \frac{\epsilon^2 + f(N, T)}{1 + f(N, T)} \quad (22)$$

where the function $f(N, T)$ is the ratio between the rigid body moments of inertia for thermal cloud and condensate and it depends only on condensate fraction, chemical potential and temperature of the Bose gas:

$$f(N, T) = \frac{\Theta_{th,rig}}{\Theta_{c,rig}} = \frac{7k_B T}{2\mu(T)} \frac{G(3)}{3G(2)} \frac{N - N_0(T)}{N_0(T)}. \quad (23)$$

Thus $f(N, T)$ resembles $\mathcal{F}(N, T)$ in Eq. 21 apart from the ratio of the squares of the scissors mode frequencies at $T = 0$ to that at T . This ratio differs significantly from unity only at temperatures $T \geq 0.6T_0$ where the thermal cloud dominates the contribution to the total moment of inertia. So we expect the static results to give a good description of the moment of inertia of the gas at all temperatures.

We can now use the analytical results obtained so far to deduce the total moment of inertia of the partially condensed system from our experiments on the scissors mode. First we can use Eqs. 14 and 13 to get the moment of inertia for the thermal and condensate *separately* from the finite temperature frequency shifts of the scissors oscillations. In Fig. 4 we show the behaviour of $\Theta'_c(T)$ (solid circles) and $\Theta'_{th}(T)$ (open circles) with temperature. Note that the moment of inertia of the thermal component is consistent with the rigid body value for all measured temperatures in the experiment $\Theta'_{therm} \approx 1$. We can see that all the relevant quantities involved in Eqs. 19 and 21 for the evaluation of the moment of inertia can be extracted from TOF images [24].

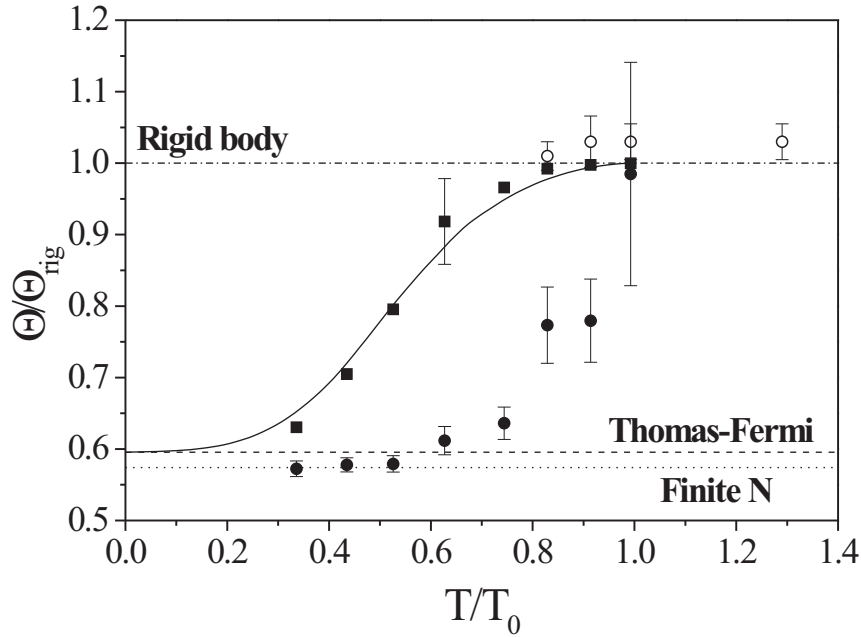


Figure 4. Reduced moment of inertia at finite temperature. Temperature dependence of the moment of inertia of the thermal (open circles) and condensed component (solid circles). The errors on these data points reflect the relative errors on the scissors mode frequencies. For low temperatures the moment of inertia of the condensate is in close agreement with the hydrodynamic prediction for our geometry (dashed line) and it is in excellent agreement with the finite number correction (dotted line). The solid line is the prediction of Eq. 22 that is based only on an estimate of the cloud widths of the interacting gas and neglects the dynamical interaction between the BEC and the thermal cloud. Finally the solid squares and line represent the moment of inertia for the total quantum gas extracted by using Eqs. 19 and 21 and the scissors mode data. The error on these data points is of the order of 7%.

The total atom number N and condensate number $N_0(T)$ are obtained from a 2D double distribution: parabolic for the BEC and Gaussian for the thermal cloud. The temperature of the cloud is deduced by fitting the wings of the thermal cloud with a 2D Gaussian distribution. The chemical potential has been deduced using the Castin-Dum equations for the expanding BEC. Using all the data extracted from the images we can ‘construct’ the moment of inertia of the total boson gas from the quadrupole Fourier signal (Eq. 19) for each measured temperature. The result is shown in Fig. 4 (solid squares) and we can compare it with the thermal and condensate contribution. The hydrodynamic prediction (dashed line) and the finite number correction (dotted line) are also shown for comparison. A theory for the scissors mode frequency has been only recently developed and also used to extract information on the moment of inertia at finite temperature [17]. Our results are consistent with a monotonic increase of the moment of inertia with increasing temperature and close to T_0 the condensate scissors

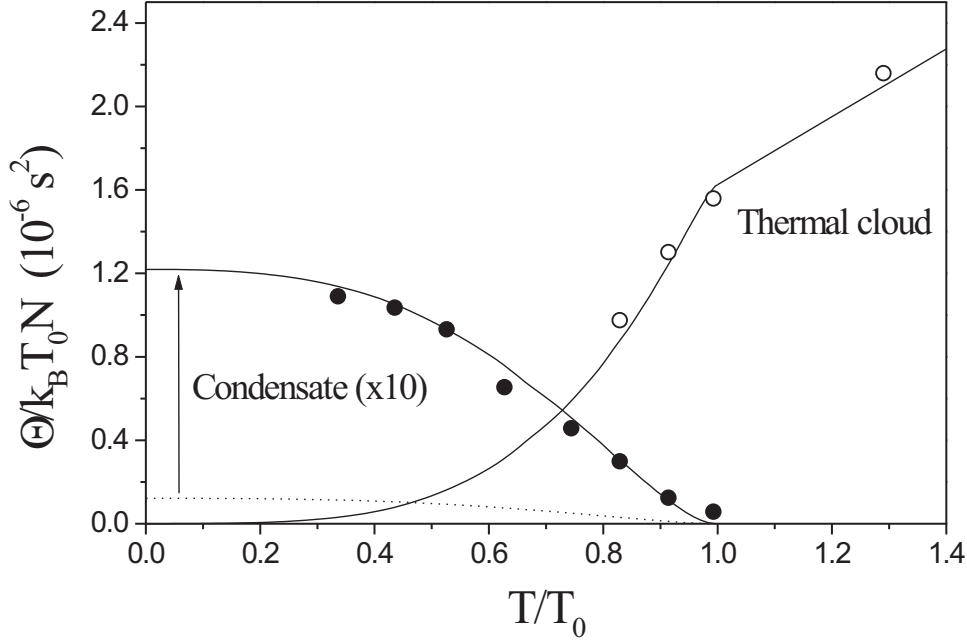


Figure 5. Temperature dependence of the absolute moment of inertia of the thermal cloud (open circles) and condensate (solid circles). The solid lines are the interacting theory predictions. The condensate data and theory have been multiplied by a factor of 10 to make them more visible. The dotted line is the original theoretical prediction for the BEC moment of inertia. The condensate and thermal component have equal moment of inertia at $T \approx 0.47 T_0$.

mode frequency correspond to an effective moment of inertia close to the rigid body value. We can also compare our approximation for the total moment of inertia with the estimate obtained from Eq. 22 using the condensate fraction for the interacting gas [25]. This is shown as the solid line in Fig. 4. Although we are neglecting the BEC scissors mode temperature frequency shift i.e. the dynamical interaction between the thermal cloud and BEC component, the agreement between the extracted data points and the static theory is good.

So far we have investigated the behaviour of the reduced moment of inertia of the gas. It is also interesting to present the data in terms of the absolute (not reduced) values of the moments of inertia for the two components of the system i.e. $\Theta_c = \Theta'_c \Theta_{c,rig}$ and $\Theta_{th} = \Theta'_{th} \Theta_{th,rig}$. In the large number limit we obtain:

$$\frac{\Theta_c}{N k_B T_0} = \Theta'_c \frac{N_0}{N} \frac{2\mu}{7 k_B T_0} \frac{\omega_x^2 + \omega_y^2}{\omega_x^2 \omega_y^2} \quad (24)$$

$$\frac{\Theta_{th}}{N k_B T_0} = \Theta'_{th} \frac{T}{T_0} \frac{N - N_0}{N} \frac{G(3)}{3G(2)} \frac{\omega_x^2 + \omega_y^2}{\omega_x^2 \omega_y^2} \quad (25)$$

In particular as a consequence of the harmonic confinement, the temperature dependence of the moment of inertia for the thermal component is linear above T_0 and behaves as $(T/T_0)^4$ below T_0 . Figure 5 shows the experimental data points and predictions based on the interacting theory for both condensate and thermal cloud absolute moment of inertia. The condensate and thermal cloud have equal moments of inertia $\Theta_c = \Theta_{th}$ at $T \approx 0.47 T_0$. At this temperature only 15% of the atoms are in the thermal cloud, but the cloud has a classical moment of inertia and a broader spatial distribution than the BEC.

4. CONCLUSIONS

In conclusion we have shown how the scissors mode is an excellent rotational probe to study the superfluid properties of a quantum gas. Specifically we have outlined its link with the moment of inertia of the gas. This allowed us to explicitly measure the quenching of the moment of inertia from our scissors mode data.

Another system where the scissors mode could be used as a powerful tool to demonstrate superfluid flow is a Fermi degenerate gas. A recent theoretical analysis [26] of that system shows that the transition to the superfluid state, below the BCS critical temperature T_{BCS} , is signaled by the disappearance of the low frequency in the scissors oscillation that occur in the normal degenerate Fermi gas above T_{BCS} . The same analysis used here for extracting the moment of inertia of the gas can be performed for a trapped Fermi gas to directly measure the quenching of its moment of inertia below T_{BCS} . In this case we have a situation similar to heavy nuclei and some theoretical predictions have been already presented in [27].

5. ACKNOWLEDGEMENTS

We would like to thank S. Stringari, F. Zambelli and N. Lo Iudice for fruitful discussions. We are also grateful to D. Cassettari and S. Cornish for comments and proof reading of the manuscript. This work was supported by the EPSRC and the TMR ‘Cold Quantum Gases’ network program (No. HPRN-CT-2000-00125). O.M. Maragò acknowledges the support of a Marie Curie Fellowship, TMR program (No. ERB FMBI-CT98-3077) and Linacre College.

6. REFERENCES

- [1] M.H. Anderson *et al.*, Science **269**, 198 (1995); K.B. Davis *et al.*, Phys. Rev. Lett. **75**, 3969 (1995).
- [2] A. J. Leggett, Rev. Mod. Phys., **71**, S318, 1999.
- [3] Eddy Timmermans, Contemp. Phys., **42**, 1, 2001; A. L. Fetter and A. A. Svidzinsky, J. Phys.: cond. matt., **13**, R135, 2001; Sandro Stringari, cond-mat/0101299, 2001.
- [4] C. Raman *et al.* Phys. Rev. Lett. **83**, 2502 (1999); A.P. Chikkatur, *et al.* Phys. Rev. Lett. **85**, 483 (2000).
- [5] M.R. Matthews *et al.* Phys. Rev. Lett. **83**, 2498 (1999).
- [6] K.W. Madison *et al.* Phys. Rev. Lett. **84**, 806 (2000).

- [7] D. Guéry-Odelin and S. Stringari, Phys. Rev. Lett. **83**, 4452 (1999).
- [8] O.M. Maragò, *et al.*, Phys. Rev. Lett. **84**, 2056 (2000).
- [9] F. Zambelli and S. Stringari, Phys. Rev. A **63**, 033602 (2001).
- [10] N. Lo Iudice and F. Palumbo, Phys. Rev. Lett. **41**, 1532 (1978); E. Lipparini and S. Stringari, Phys. Lett. **130B**, 139 (1983).
- [11] D. Bohle, A. Richter, W. Steffen, A.E.L. Dieperink, N. Lo Iudice, F. Palumbo, and O. Scholten, Phys. Lett. **137B**, 27 (1984).
- [12] N. Lo Iudice, Phys. Part. Nucl., **28**, 556(1997) and Rivista del Nuovo Cimento, **23**, 1(2000).
- [13] F. Dalfvo *et al.*, Rev. Mod. Phys. **71**, 463(1999).
- [14] H. Lamb, *Hydrodynamics*, Cambridge University press (1906).
- [15] Onofrio Maragò *et al.*, Phys. Rev. Lett. **86**, 3938 (2001).
- [16] M.O. da C. Pires and E.J.V. de Passos, J.Phys.B. **33** 3929 (2000).
- [17] B. Jackson and E. Zaremba, cond-mat/0105465 (2001); B. Jackson and E. Zaremba, cond-mat/0106652 (2001).
- [18] D. S. Jin *et al.*, Phys. Rev. Lett. **77**, 420 (1996); M.-O. Mewes *et al.*, Phys. Rev. Lett. **77**, 988 (1996).
- [19] K. Huang, *Statistical mechanics*, Wiley, 2nd Ed., (1987).
- [20] A. Bohr and B. Mottelson, *Nuclear Structure*, Benjamin - New York, vol. 2, (1975).
- [21] D. Pines and P. Nozières, *The theory of quantum liquids*, Benjamin - New York, (1966).
- [22] The angular momentum evolution for a quantum system is in general given by the Heisenberg equation of motion $d\vec{J}/dt = -i[\vec{J}, H]/\hbar$. During a scissors mode oscillation the angular momentum is intrinsically linked to the quadrupole moment. Thus if we excite the xz scissors mode, then using relation 11, we can write the evolution of the relevant averaged component $\langle J_y \rangle$ of the angular momentum $d\langle J_y \rangle/dt = -m(\omega_z^2 - \omega_x^2)\langle Q \rangle = -mN(\omega_z^2 - \omega_x^2)\langle x^2 - z^2 \rangle \theta(t)$. From the scissors mode angle evolution we can easily integrate the previous equation and using the Thomas-Fermi mean square widths we finally get the explicit evolution of the angular momentum:

$$\langle J_y \rangle = -\frac{2\theta_0\mu N}{7\omega_{sc}} \frac{(\omega_z^2 - \omega_x^2)^2}{\omega_x^2\omega_z^2} \sin(\omega_{sc}t).$$

During a scissors mode oscillation the angular momentum oscillates at the scissors mode frequency and out of phase with respect to the scissors mode angle.

- [23] S. Stringari, Phys. Rev. Lett. **76**, 1405 (1996).
- [24] Onofrio Maragò, D.Phil. Thesis, University of Oxford (2001).
- [25] A. Minguzzi *et al.*, J. Phys. (Condens. Matter) **9**, (1997) L33-L38.
- [26] A. Minguzzi and M.P. Tosi, Phys. Rev. A **63**, 023609, (2001).
- [27] M. Farine and P. Schuck and X. Vinas, Phys. Rev. A **62**, 013608, (2000).